

## **FINAL REPORT**

### **ASSESSMENT OF SUPERSONIC JET IMPINGEMENT ON MLP SURFACE USING EXPERIMENTAL COLD FLOW TEST AND COMPARISON WITH CFD**

**SUBMITTED BY:**

SAKSHI VERMA

PROJECT TRAINEE

NATIONAL INSTITUTE OF TECHNOLOGY SIKKIM

SOLID MOTOR PERFORMANCE AND ENVIRONMENT TEST FACILITY

(SMP & ETF)

**UNDER THE GUIDANCE AND SUPPORT OF:**

G.VENKATESH

Dy. MANAGER, AAT&HATF

SMP&ETF



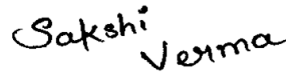
**INDIAN SPACE RESEARCH ORGANISATION**

**SATISH DHAWAN SPACE CENTRE (SDSC)**

**SHAR, SRIHARIKOTA ANDHRA PRADESH**

**1. Title:** Supersonic Jet Impingement on MLP Surface Using Experimental Cold Flow Test and Comparison With CFD.

**2. Prepared by**



SAKSHI VERMA

**3. Approved by**



G Venkatesh  
Dy.Manager, HATF/SMPTF



T Srinivasreddy  
Manager, E&HATF

**No. of pages**

**33**

**No. of tables**

**6**

**No. of figures**

**18**

**No. of reference**

**10**

**Abstract:**

Extensive environmental testing of rocket exhaust nozzles is required to assess the impact of rocket exhaust on the launch structure. The Mobile Launch Platform (MLP) is subjected to strong aero-thermal forces from the solid rocket motors, which might damage the top surface. The study entailed doing Computational Fluid Dynamics (CFD) analysis at a lower 1:100 scaling ratio while employing a 1:50 scaled launch vehicle model. Gaseous nitrogen with a specific heat ratio of 1.4 was used in cold flow testing. It was possible to get important insights by contrasting CFD analysis and experimental findings, which enhanced the design standards for the launch structure. The goal of this research was to improve design, resulting in a launch structure that is more reliable and appropriate.

**Keywords:** Mobile Launch Platform (MLP), Supersonic Jet Impingement, Cold Flow Test, Flow Structure of Jet Impingement, CFD Analysis

## DECLARATION

I solemnly declare that the research work presented and carried out is the result of my dedicated efforts as a research trainee. I would like to acknowledge and express my heartfelt gratitude to ISRO (Indian Space Research Organisation) for their invaluable contributions to my learning experience.

During my tenure as a research trainee at SMP&ETF ISRO, I had the privilege of working alongside distinguished scientists, researchers, and experts in various fields. Their guidance, mentorship, and extensive knowledge have played a pivotal role in shaping my understanding of research methodologies, experimental techniques, and scientific principles.

The research environment at SMP&ETF ISRO provided me with all facilities for exploring things. I was fortunate to engage in intellectually stimulating discussions and workshops that broadened my horizons and deepened my insights into the field of Supersonic Impinging Jet.

Furthermore, the valuable feedback, constructive criticism, and continuous support received from the researchers and staff at SMP&ETF ISRO were instrumental in refining my research work and enhancing its quality. Their expertise and unwavering commitment to excellence have significantly contributed to the overall outcome of this publication.

I would like to extend my heartfelt appreciation to the management and administration of SMP&ETF ISRO for allowing me to be a part of their esteemed organization. The platform offered by SMP&ETF ISRO has been instrumental in shaping my research skills, fostering my scientific curiosity, and nurturing my professional growth.

I would also like to express my gratitude to my fellow research trainees and colleagues at SMP&ETF ISRO for their collaboration, camaraderie, and intellectual exchanges, which have greatly enriched my research experience. The vibrant research community at SMP&ETF ISRO has been an endless source of inspiration and motivation throughout this journey.

In conclusion, I hereby affirm that without the support, guidance, and resources provided by SMP&ETF ISRO, this research work would not have been

possible. Therefore, I acknowledge and attribute a significant portion of my learning experience to the invaluable contributions of SMP&ETF ISRO.

**Sakshi Verma**

**National Institute of Technology Sikkim**

**Mechanical Engineering**

# **ACKNOWLEDGEMENT**

I would like to take this opportunity to express my sincerest appreciation and gratitude to all the individuals who contributed to the successful completion of the project conducted at SMP&ETF ISRO. Their dedication and hard work were instrumental in achieving my goal.

First and foremost, I am immensely grateful to my Mentor, Venkatesh Sir, for his exceptional guidance throughout the project. His expertise and insights provided invaluable perspectives and helped shape the project's direction. I am very thankful to him for giving me the spirit of new knowledge, enthusiasm, and dedication to working in this field as a researcher in the future.

His practical knowledge and expertise greatly contributed to the project's execution, and I am grateful for his support throughout the duration. I am grateful that I paved the way to build up the foundations for my research career under his guidance.

The unwavering support and encouragement from everyone involved provided me with the necessary resources and opportunities to enhance my knowledge and gain valuable exposure to an industrial environment. I am grateful for the trust placed in me and for providing a platform to explore innovative ideas.

I would also like to thank Aditya Sir and Deepthi Ma'am for constantly guiding and supporting me to achieve and address all the problems from scratch faced during the project.

In conclusion, I want to express my deep gratitude to all those who played a direct or indirect role in the successful completion of this project. Your contributions, support, and encouragement have been invaluable. I am truly honored to have worked with such remarkable individuals, and I am confident that the skills and experiences gained during this project will have a lasting impact on my personal and professional development.

**Sakshi Verma**

**National Institute of Technology Sikkim**

**Mechanical Engineering**

## TABLE OF CONTENTS

<b>1. ABSTRACT .....</b>	<b>7</b>
<b>2. INTRODUCTION.....</b>	<b>8</b>
<b>3. OBJECTIVE .....</b>	<b>10</b>
<b>4. FUNDAMENTAL OF SUPERSONIC FLOW .....</b>	<b>11</b>
<b>5. CONVERGENT-DIVERGENT NOZZLE.....</b>	<b>12</b>
<b>6. THE OCCURRENCE OF STAGNATION BUBBLES IN SUPERSONIC IMPINGEMENT FLOWS .....</b>	<b>17</b>
<b>7. MODELS DETAILS AND EXPERIMENTAL SETUP .....</b>	<b>18</b>
i) Cold Flow Test .....	18
ii) Mobile Launch Platform (MLP) .....	18
iii) Flow Visualization .....	19
iv) Nozzle and Flow Condition .....	20
v) Geometry .....	21
vi) Meshing.....	22
vii) Ansys Fluent Set Up .....	24
<b>8. EXPERIMENTAL ANALYSIS.....</b>	<b>25</b>
<b>9. NUMERICAL SIMULATION RESULTS .....</b>	<b>26</b>
i) Residuals .....	27
ii) Pressure Contour .....	27
iii) Temperature Contour .....	29
iv) Velocity Contour.....	31
<b>10. CONCLUSION .....</b>	<b>32</b>
<b>11. REFERENCE.....</b>	<b>33</b>

## ABSTRACT

This project aims to provide the analysis of such jets by conducting pressure measurements on the surface at a 1:100 scaled model. Additionally, computational fluid dynamics (CFD) simulations using ANSYS Workbench are performed to enhance the data obtained. A cold flow test is conducted on a Mobile Launch Platform (MLP) to assess the practical implications of the findings.

The primary objective of this experiment is to investigate the complex flow behavior of supersonic-impinging jets. Taking a 1:100 scaled 2D axisymmetric model, we aim to determine the optimal scale for pressure measurements on a flat surface.

The pressure measurements are conducted at a 1:50 scale, providing crucial data on pressure distributions, and flow velocities. These measurements serve as a foundation for further analysis and understanding of impinging jet dynamics.

CFD simulations are performed using ANSYS Workbench, allowing for a detailed investigation of the fluid flow characteristics at the 1:50 scale. The CFD results supplement the experimental data, facilitating a more comprehensive flow analysis.

To achieve greater accuracy and finer details in the flow characteristics, the scaled model is reduced to 1:100 in the subsequent phase. The refined data obtained at this scale offers deeper insights into the impinging jet behavior.

Gaseous nitrogen with a specific heat ratio of 1.4 was used in cold flow testing. Geometric and Kinematic dimensional similarity is used in this experiment for providing us with the benefit of studying the prototype. A cold flow test is conducted on MLP, emulating real-world conditions during launch preparations.

# INTRODUCTION

It is crucial to inspect the Mobile Launchpad (MLP) and Umbilical Tower for structural integrity before launching a vehicle. Aerothermodynamic loads and aeroacoustics loads that a supersonic nozzle applies on the pad and the tower are the two major types of loads that the MLP in which a rocket is maintained must contend with. The pressure loads that are being imparted by the same will be the main emphasis of this paper. These stresses should be taken into account throughout the MLP's development phase to accurately identify the launch pad and umbilical tower structural failure zones. By using the general scenario of thermodynamic loads imposed by a supersonic impingement on a flat plate wall, these loads are simple to illustrate. This application's primary goal is to look into how jet plumes affect a deflector. To accurately measure the pressure applied at various positions on the MLP using pressure-measuring sensors at varying L/De ratios, the test was conducted utilizing cold flow conditions of a 1:100 model of SSLV lift-off boosters. A CFD simulation has been developed for the experimental example and will be detailed in due time. For the simulation, we used ANSYS Inc. student workbench software. Large rockets are typically launched from large structures known as launchpads; in our instance, the launchpad is referred to as the Mobile Launchpad (MLP). Most of these MLPs include perforations that allow rocket plumes to pass through them and impact the jet deflector that is positioned beneath the MLP. The weight that a rocket places on the launch pad and all of its supporting structures primarily depend on the height at which the rocket is located. The plumes typically interact with the current jet deflectors. The launch platform and deflector gradually come into contact with the plumes during the flight's ascent. Further, ascent essentially constitutes a free jet state because it has no longer any impact on the platform. A complex flow structure generally forms when plumes impinge on a flat surface like a launch platform.

The analysis of the test was conducted using a scaled model of the Launch vehicle, with a scale of 1:100. The model accurately represented the real-life case for simulation purposes. By using the correct geometry in the computational fluid dynamics (CFD) analysis, we were able to gain insights into the current scenario.



In the simulation, a secondary flow was not considered. Instead, dimensional analysis was employed to establish a scaling law that enabled us to extrapolate information from the small model to design a larger prototype. According to the principle of similarity, flow conditions for the model and prototype are considered similar if all relevant dimensionless parameters have the same values for both.

The geometric similarity was used in this experiment, suggesting that all dimensions were reduced at a linear scale ratio while preserving angles and flow directions without altering the orientation of the model and the prototype. Additionally, kinematic similarity played a role, ensuring that the motion of the two systems was similar, with corresponding particles occupying corresponding positions at corresponding times. This allowed us to maintain a constant nozzle exit Mach number and chamber pressure.

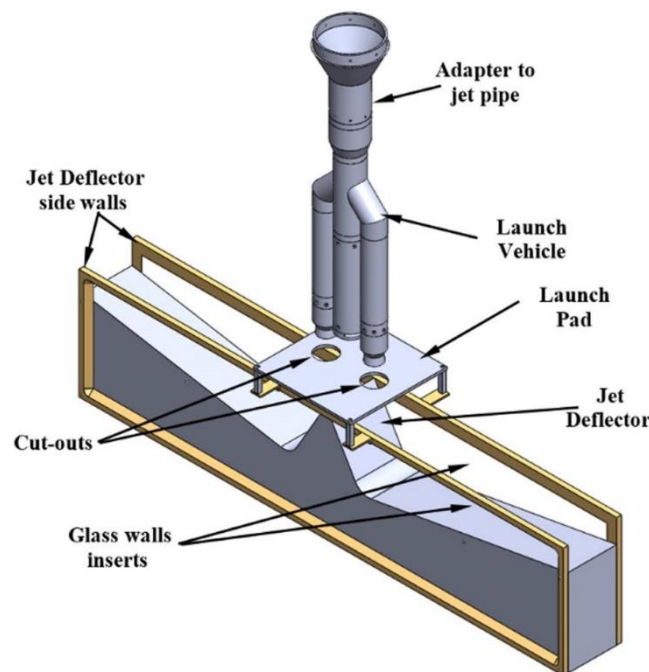


**Fig.1. Launchpad Structure**

## OBJECTIVE

Scientists have realized the value of precisely calculating the practicality of launch structures to create extremely effective ones. In this sense, computational fluid dynamics (CFD) analysis has shown to be a useful technique. However, it is important to recognize that CFD might not completely compare with actual test settings.

An experimental method was used to close the gap between simulation and reality. The goal of this experiment was to gauge the launch pressure of a launch vehicle that was scaled down to 1:50. The information gathered from this experiment is crucial for determining the precise location where loads should be applied to the launch structure.

This experiment has grown to be especially important for performing a thorough examination of the pressure loads caused by a supersonic jet impingement on a flat plate. Designing launch structures that can resist and function at their peak during the rigorous lift-off period requires a thorough understanding of these pressure loads.

An ANSYS Workbench 1:100 scale model of the launch vehicle environment was used to conduct the CFD investigation. The CFD results have given important insights into the pressure distribution and flow behavior inside the launch environment, while not being directly equivalent to the experimental size.

An effective synergy is created when experimental data and CFD findings are combined. Engineers can get a thorough grasp of how the launch structure performs in actual use by correlating and confirming the data. This comprehensive method makes it possible to forecast the dynamics of the full-scale launch environment, which aids in the creation of reliable and effective launch structures.

# 1. Fundamentals of Supersonic Flow

Bernoulli's equation, which describes the connection between pressure and velocity in a flowing fluid, is one of the most fundamental in fluid dynamics. It is mentioned frequently when describing how aircraft wings produce lift since it is so crucial to aerodynamics. Bernoulli's equation is a specific application of energy conservation to a fluid with constant density rather than a fundamental equation of aerodynamics.

Five fundamental equations, of which Bernoulli's equation is a special example under the assumptions of constant density, are used to describe the fluid dynamics and thermodynamics of compressible flow. For illustration, let's assume that any flow of a fluid with an arbitrary control volume is

- The control volume is adiabatic, which means that no heat is transferred from or into it.
- inviscid, which means there is no friction.
- at constant energy, i.e., without any external effort being applied to the fluid (like through a compressor).

This type of flow is isentropic flow (constant enthalpy).

Five basic conservation equations—density ( $\rho$ ), pressure ( $p$ ), velocity ( $v$ ), area ( $A$ ), mass flow rate ( $\dot{m}$ ), temperature ( $T$ ), and entropy ( $s$ )—rule the isentropic flow illustrated above.

This means that the following expressions must hold at the flow's two stations, 1, and 2, respectively.

- Conservation of mass:  $\dot{m}_1 = \dot{m}_2 \Rightarrow \rho_1 v_1 A_1 = \rho_2 v_2 A_2$
- Conservation of linear momentum:  $dF = d(ma) = \dot{m} dv \Rightarrow p_1 A_1 - p_2 A_2 = \dot{m} (v_2 - v_1)$
- Conservation of energy:  $T_1 + \frac{v_1^2}{2c_p} = T_2 + \frac{v_2^2}{2c_p} = \text{constant}$
- Equation of state:  $p = \rho RT$
- Conservation of entropy (in adiabatic and inviscid flow only):  $s_1 = s_2$

## 2. Convergent-Divergent Nozzle

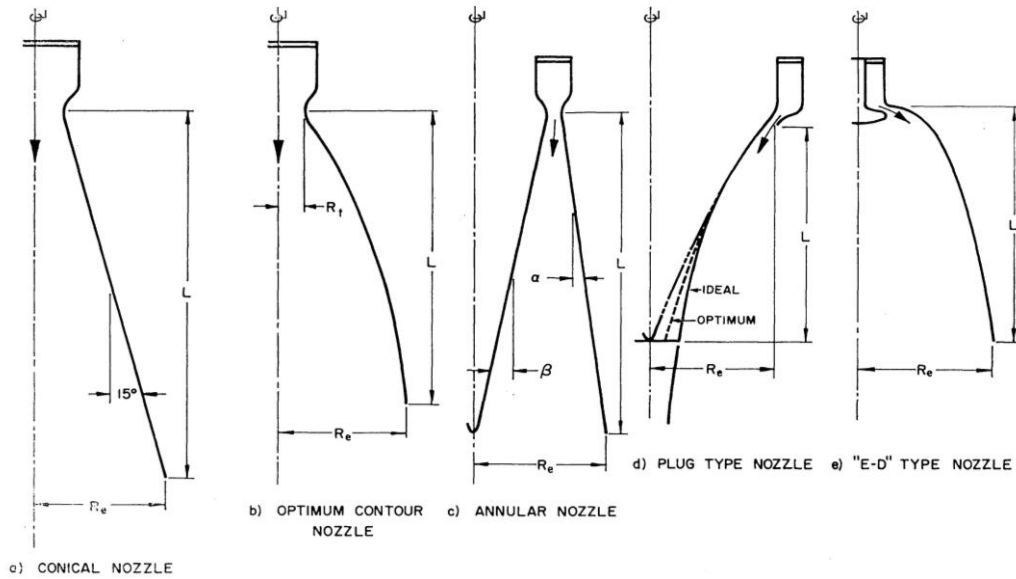


**Fig.2. Various types of rocket nozzle**

The performance of rocket engines is highly dependent on the aerodynamic design of the expansion nozzle, the main design parameters being the contour shape and the area ratio. The nozzle is the part of the rocket engine extending beyond the combustion chamber. Typically, the combustion chamber is a constant-diameter duct into which propellants are injected, mixed, and burned for a sufficiently long time to allow complete combustion of the propellants before the nozzle accelerates the gas products. The nozzle is said to begin at the point where the chamber diameter begins to decrease.

Simply stated, the nozzle uses the stagnation temperature  $T_0$  and pressure  $p_0$  generated in the combustion chamber to induce thrust by accelerating the combustion gas to a high supersonic velocity. For a given stagnation state, the nozzle exits velocity  $v_e$  that can be achieved is governed by the nozzle expansion ratio, defined as the ratio between the nozzle exit area and throat area,  $A_e / A_t$ . The thrust  $F$  produced by the nozzle can be expressed as

$$F = \dot{m}v_2 + (p_2 - p_3)A_2$$

where  $\dot{m}$  is the mass flow through the nozzle and  $v_e$ ,  $p_e$ , and  $A_e$  are the velocity, pressure, and cross-sectional area at the nozzle exit, respectively, and  $p_a$  is the ambient pressure. Optimum thrust is obtained when the nozzle exit pressure is

adapted to the atmospheric pressure,  $p_e = p_a$  (so-called adapted or ideally expanded flow).

From ground level up to this altitude, the flow is over-expanded, i.e.,  $p_a > p_e$ , while it is under-expanded ( $p_a < p_e$ ) at higher altitudes. It is to allow the nozzle to operate in a state of flow separation. In principle, a first or main-stage rocket nozzle could be designed for much higher area ratios than those commonly used today, thereby achieving higher performance at high altitudes, where the main part of the trajectory takes place.

The chamber temperature  $T_1$  is at the nozzle inlet and, under isentropic conditions, differs little from the stagnation temperature from the combustion temperature. This leads to an important simplified expression of the exhaust velocity  $v_2$ .

$$\begin{aligned} v_2 &= \sqrt{\frac{2k}{k-1} R T_1 \left[ 1 - \left( \frac{p_2}{p_1} \right)^{(k-1)/k} \right]} \\ &= \sqrt{\frac{2k}{k-1} \frac{R' T_0}{\mathfrak{M}} \left[ 1 - \left( \frac{p_2}{p_1} \right)^{(k-1)/k} \right]} \end{aligned}$$

The area ratio for a nozzle with the isentropic flow can be expressed in terms of Mach numbers for any points  $x$  and  $y$  within the nozzle. This relationship, along with those for the ratios  $T/T_0$  and  $P/P_0$ , for  $A_x = A_t$  and  $M_x = 1.0$ .

$$\frac{A_y}{A_x} = \frac{M_x}{M_y} \sqrt{\left\{ \frac{1 + [(k-1)/2] M_y^2}{1 + [(k-1)/2] M_x^2} \right\}^{(k+1)/(k-1)}}$$

The stagnation pressure during an adiabatic nozzle expansion remains constant only for isentropic flows. It can be computed from

$$p_0 = p \left[ 1 + \frac{1}{2} (k-1) M^2 \right]^{k/(k-1)}$$

The relation between stagnation temperature and Mach number can now be written from

$$T_0 = T \left[ 1 + \frac{1}{2} (k-1) M^2 \right]$$

By the using equation we calculate the impingement pressure, temperature, and thrust forces.

We may demonstrate how the following equation relates the change in speed to the change in area:

$$(M^2 - 1) \frac{dv}{v} = \frac{dA}{A}$$

Some intriguing characteristics of compressible flow can be discovered without solving this equation for a particular issue:

- For subsonic flow, or  $M < 1$ , and a positive constant for  $c$ . A decrease in cross-sectional area is required to increase flow velocity, and vice versa.
- In the case of sonic flow,  $M = 1$ . The area must be at a minimum for sonic flow since  $A$  must be finite.
- for supersonic flow, or  $M > 1$ . In other words, increasing the cross-sectional area without raising the flow velocity is not conceivable.

To expand gas from subsonic to supersonic speeds, the flow must first travel to Mach 1 in a convergent nozzle and then expand through a divergent nozzle. Rocket engines always feature enormous bell-shaped nozzles to expand the exhaust gases into supersonic jets because the flow must be sonic at the point of minimum area, called the throat.

The pressure differential between the combustion chamber and the nozzle exit propels the flow through such a coaxial-shaped convergent-divergent nozzle. The gas is essentially at rest and stagnation pressure in the combustion chamber. The gas usually moves and is at a lower pressure when it leaves the nozzle. The first crucial need for producing supersonic flow is a high enough pressure ratio between the combustion chamber and the nozzle throat to ensure that the flow is sonic at the throat. Supersonic flow cannot exist in the diverging region of the nozzle without this crucial condition at the throat.

From the connection between pressure and Mach number shown above, we can calculate this precise pressure ratio for dry air ( $\gamma = 1.4$ ):

$$\frac{p_t}{p} = \left(1 + \frac{\gamma-1}{2} M^2\right)^{\frac{\gamma}{\gamma-1}} = \left(\frac{\gamma+1}{2} M^2\right)^{\frac{\gamma}{\gamma-1}} = 1.893$$

A pressure ratio greater than or equal to 1.893 is needed to ensure sonic flow at the throat. In this situation, the temperature would be:

$$\frac{T_t}{T} = 1 + \frac{\gamma-1}{2} 1^2 = 1.2$$

or 1.2 times lower than the combustion chamber's temperature (assuming no heat is lost, or work is done in the interim, i.e., isentropic flow)

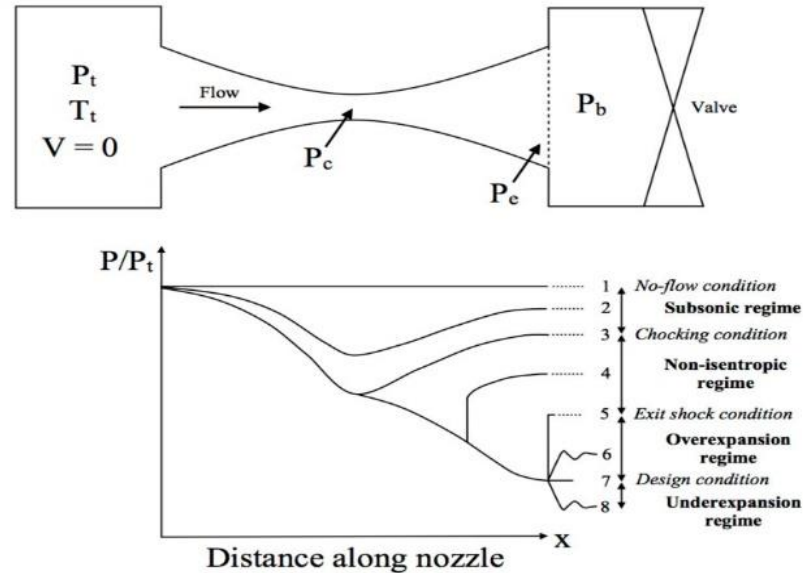


**Fig.3. Flow Visualization**

At a certain stagnation temperature  $T_t$  and pressure  $P_t$ , the gas in the upstream reservoir is at rest. A valve can be used to control the back pressure or  $P_b$ , in the reservoir upstream. The pressure at the point of the minimal area within the nozzle is known as the throat pressure  $P_c$ , whereas the pressure at the exit plane of the diverging portion of the nozzle is known as the exit pressure  $P_e$ . The change of pressure across the nozzle is affected by changing the back pressure  $P_b$ , as seen in the figure above. There are some possible exit plane circumstances based on the back pressure.

1. The valve is closed under the **no-flow** situation, and  $P_b = P_e = P_c = P_t$ . This is the uninteresting circumstance when nothing noteworthy occurs. Without flow, nothing.
2. **Subsonic flow regime:** The valve is partially open, causing the nozzle to operate in subsonic flow. The pressure decreases from the upstream reservoir to a minimum at the throat (where Mach 1 is not reached due to a pressure ratio of 1.893). Subsequently, the flow in the diverging part slows down, and the pressure increases. The back pressure and exit pressure ( $P_e$ ) are the same.

3. **Critical back pressure:** The back pressure has now reached a point where it is so low that the flow at the throat may approach Mach 1.  $P_t/P_c$  thus is 1.893. Although the flow does not reach supersonic levels, the divergent portion of the nozzle continues to function as a diffuser because the exit flow pressure ( $P_e = P_b$ ) is still equal to the back pressure. The maximum mass flow rate has been reached, and the nozzle is now blocked, however, the flow cannot move faster than Mach 1 at the throat.
4. **Non-isentropic flow regime:** Reducing back pressure accelerates flow to supersonic speeds in the divergent nozzle after reaching Mach 1 at the throat. The nozzle gets choked, and the convergent part's flow remains the same. A shock wave forms within the divergent section, causing a supersonic-to-subsonic transition. Diverging nozzle further diffuses flow to balance exit and back pressures ( $P_e = P_b$ ). Shock wave moves downstream faster and becomes more severe with decreasing back pressure. Shock waves are always positioned within divergent portions to balance exit and back pressures.
5. **Over-expanded flow regime:** With extremely low back pressure, the flow is supersonic in the entire divergent part, subsonic in the convergent part, and sonic at the throat. This overexpansion leads to sudden constriction after nozzle exit due to lower exit pressure than gas pressure. Our simple 1D flow assumptions cannot simulate the non-isentropic oblique pressure waves resulting from these rapid compressions.
6. On contrary to the over-expansion regime, the back pressure is now lower than the supersonic flow's exit pressure, causing the exit flow to expand to synchronize with the reservoir pressure. Again, in this instance, oblique pressure waves that expand outward rather than compress inward control the flow.



### **3. The Occurrence of Stagnation Bubbles in Supersonic Impingement Flows**

Supersonic jets are produced in a variety of high-pressure gas environments, including the exhaust from rocket motors. Severe aerodynamic and thermal stresses may be generated if these jets collide with solid things like the ground. One such phenomenon is a curious shock layer stagnation bubble that lies on the influences on the distribution of heat transfer and pressure on the surface where the wall jet extends its flow.

In any shock configuration resulting from the normal impingement of an axisymmetric, supersonic jet on a flat plate, the central shock must be normal at the axis because of symmetry. One, therefore, expects to find that the pressure at the jet axis on the plate is equal to the value of the pitot pressure immediately upstream of the central point on the shock. The center point on the plate is then the point of maximum plate pressure. The maximum pressure measured on the plate occurs off the center and the pressure measured at the center of the plate is less than the normal shock recovery pressure. Such pressure distributions have all been interpreted as indicating the presence of a bubble of slowly recirculating fluid in the shock layer. The diameter of this bubble may be up to 0.8 times the jet diameter and its height may be large enough to force the plate shock to assume a peaked shape.

There appear to be two classes of situations in which bubbles occur.

One is at moderate plate displacements in under-expanded jets, the other is at small plate displacements in certain under-expanded jets and certain nominally uniform jets. A plausible explanation exists for the existence of bubbles in the first class of cases, but none has so far been put forward for the second. The probe measurements suggest that Mach numbers up to about 0.4 are achieved in the bubble.

It has been shown that the bubbles sometimes encountered in the shock layers of nominally uniform supersonic jets impinging on perpendicular flat plates are caused by weak shock waves originating either from small imperfections in the nozzle wall or from a slightly inaccurate design or production of the nozzle contour. The bubbles can be eliminated by suitable improvements to the nozzle. Since the shock waves responsible are very weak, their intersections with the

plate shock must occur close to the axis. This in turn means that the flow pattern with a given nozzle is very sensitive to plate position.

## **4. Model Details and Experimental Set Up**

### **1. Cold flow test:**

The primary purpose behind including cold flow testing in the experimental setup is to save costs, improve safety, and yet have a reliable way to imitate real-world climatic conditions. These tests provide an easy approach to simulating critical operating conditions with less uncertainty, permitting alterations that are diagnostic-friendly.

The working fluid for this particular experiment is nitrogen gas, which is extensively used for experiments and is easily accessible in its pure state. Among its advantageous characteristics are a molar mass of 28 g/mol and a specific heat ratio of 1.4. The small weight of the gas ensures easy handling and manipulation during the experiment setup, which is a considerable benefit.

Additionally, nitrogen is an inert gas, which makes it suitable for use in subsequent experiments on the same workstation because it has no negative effects and does not interact chemically with the nozzle wall. The gas is a great option for obtaining the target nozzle exit temperature of 86.9 K because it also undergoes the procedure with little temperature rise.

This cold flow test accomplishes several goals by using nitrogen gas as the working fluid: it offers a realistic and economical depiction of real-world circumstances, assures safety in the experimental setting, and enables excellent diagnostic assessments.

### **2. Mobile Launch Pad (MLP):**

Large rockets are typically launched from large structures known as launchpads; in our instance, the launchpad is referred to as the Mobile Launchpad (MLP). Most of these MLPs include perforations that allow rocket plumes to pass through them and impact the jet deflector that is positioned beneath the MLP. The Mobile Launcher is a very large heavy beam/truss steel structure designed to support the Launch vehicle during

its buildup and integration in the Vehicle Assembly Building, transportation from the Vehicle Assembly Building out to the launch pad, and providing the launch platform at the launch pad.



**Fig.4. Mobile Launch Pad (MLP)**

### **3. Flow Visualization:**

Flow structures in the free jet region resemble a similar feature as in the free jet under the same nozzle operational conditions. For an under-expanded jet, the flow expands at first until its pressure balances with the ambient pressure. Then, the flow becomes over-expanded and induces compression waves, which converge to form the intercepting shocks. For an overexpanded jet, in other words, the pressure at the nozzle exit is lower than ambient pressure, oblique shocks would be generated by the compression from the surrounding fluid. For an ideally expanded jet, the oblique shocks become weaker and are not as distinguishable as in the overexpanded case. The velocity difference across the pressure-balanced boundary creates a shear layer (or mixing layer), which tends to grow downstream. At the same time, the incident oblique shocks reflect at certain points along the jet axis. Structures of the reflected shocks may resemble an X shape (or a conical shape) if the reflection is regular, or a Mach disk if the reflection is singular. Slipstreams would appear at the triple points, where the incident shocks, the reflected shocks, and the Mach disk intersect. When the jet is not extremely under-expanded, quasi-periodic shock cells could appear repeatedly. The shear layers would merge at the jet axis as the jet develops downstream, causing nearfield shock structures to disappear and hence the potential core of the

jet ends. When the impinged plate is near the potential core, there would be further interaction between the impinging jet and the plate.

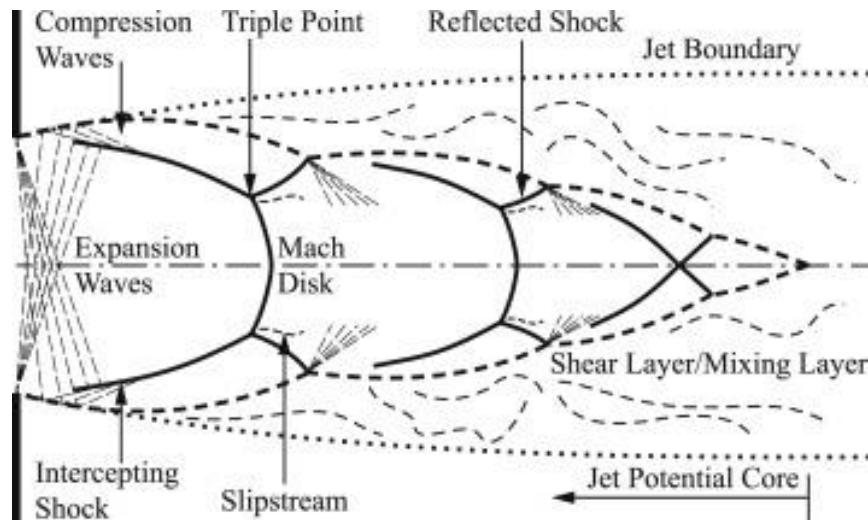


**Fig.5. Scheme of a moderately under-expanded free jet**

#### **4. Nozzle and Flow conditions:**

In this experiment, we are obtaining radial pressure distributions at various axial distances due to the impingement of high velocity and high temperatures rocket exhaust gases generated by burning nitrogen. The contour nozzle used in the experiment was a shortened version of the contour corresponding to  $M=3.5$ . The analysis of the test was conducted using a scaled model of the Launch vehicle, with a scale of 1:100. This contour was designed by the method of characteristics for a constant value of  $\gamma=1.4$ . In these cases, the nozzle used for model tests had a throat diameter of 8.445 mm. and an area ratio of 6.79. The divergent portion of the contour nozzle had an initial divergence angle of  $15^\circ$ . The exit diameter of the nozzle is 22 mm, and the exit temperature consists of 86.9 K. This experiment is set up at different  $L/D_e$  ratios 4, 5, and 6 respectively.

**Table 1. Nozzle Parameters**

SL NO.	PARAMETERS	HOT FLOW	COLD FLOW	UNITS
1	Area Ratio	13.7	6.79	NA
2	Nozzle Exit Diameter	2200	44	mm
3	Nozzle Throat Diameter	594	16.89	mm
4	Nozzle Inlet Diameter	2000	40	mm
5	Exit Mach Number	3.5	3.5	NA
6	Specific heat ratio	1.19	1.4	NA
7	Chamber Pressure	51	32.03	bar
8	Mass flow rate	900	1.674	kg/s
9	Molar Mass	29	28	g/mol
10	Exit Temperature	1575	86.9	K

## 5. Geometry:

The dimensional analysis provides us with a scaling law that helps us to take information from a small model to design a much larger prototype. Similarity tells us that flow conditions for a model and prototype are similar if all relevant dimensionless parameters have the same values for the model and the parameter. For this experiment, we have used geometric\_similarity and kinematic\_similarity for making this model, and this suggests we reduce all dimensions at a linear scale ratio, and it helped us to keep the nozzle exit Mach Number and chamber pressure constant. The analysis of the test was conducted using a scaled model of the Launch vehicle, with a scale of 1:100.

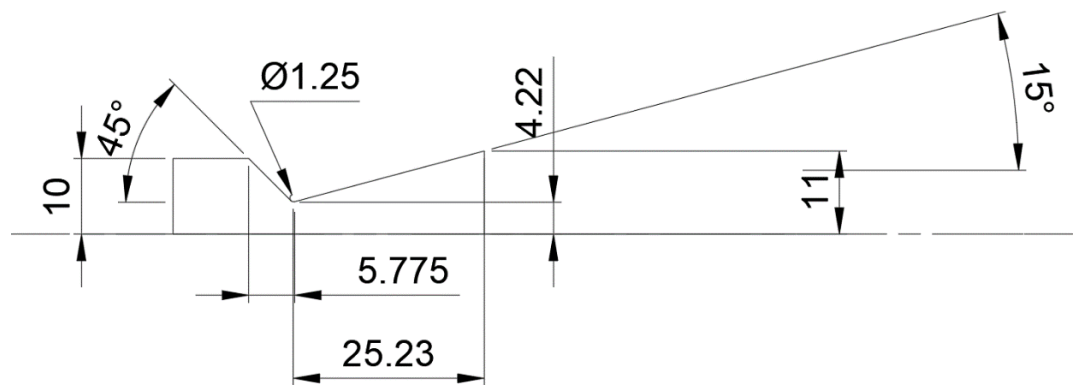


Fig.6. Nozzle (All dimensions in mm)

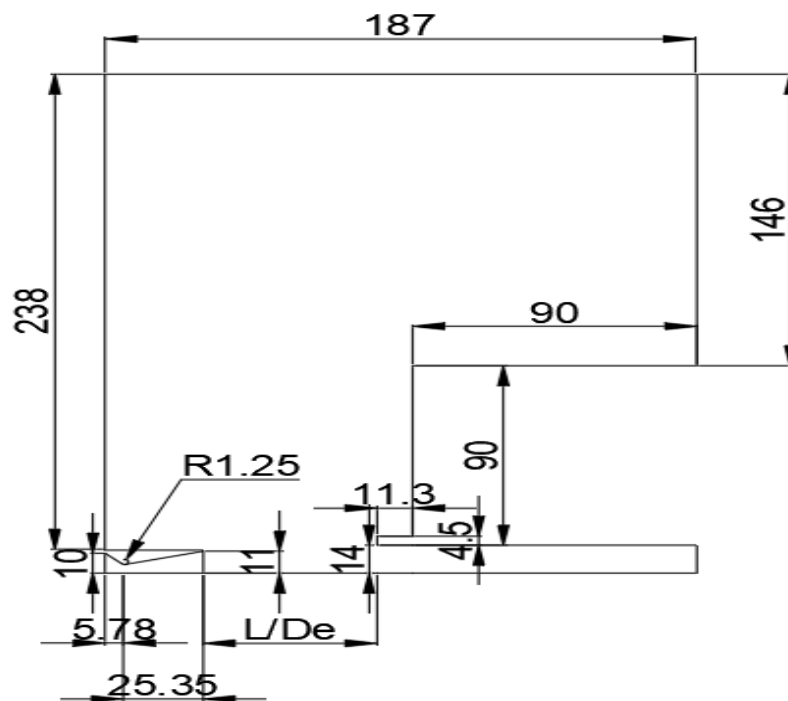


Fig.7. Overall Geometry (All dimensions in mm)

## 6. Meshing:

Meshing in ANSYS entails discrete the computational domain into smaller components. For precise simulations and reliable findings, a suitable mesh is essential. It guarantees that flow or structural aspects are sufficiently resolved. There are different respects  $L/De$  ratio have different number of nodes and elements.

**Table 2. Meshing**

SL. NO.	RATIO	NO. OF NODES	NO. OF ELEMENTS
1	2	77579	76433
2	4	84390	83261
3	6	61162	29958

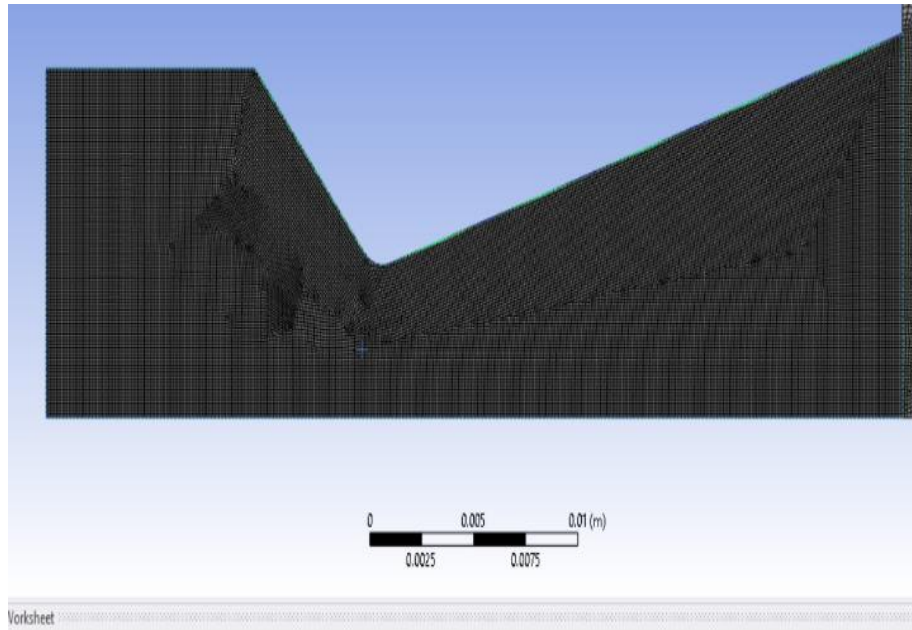


**Fig.8. Nozzle Meshing**

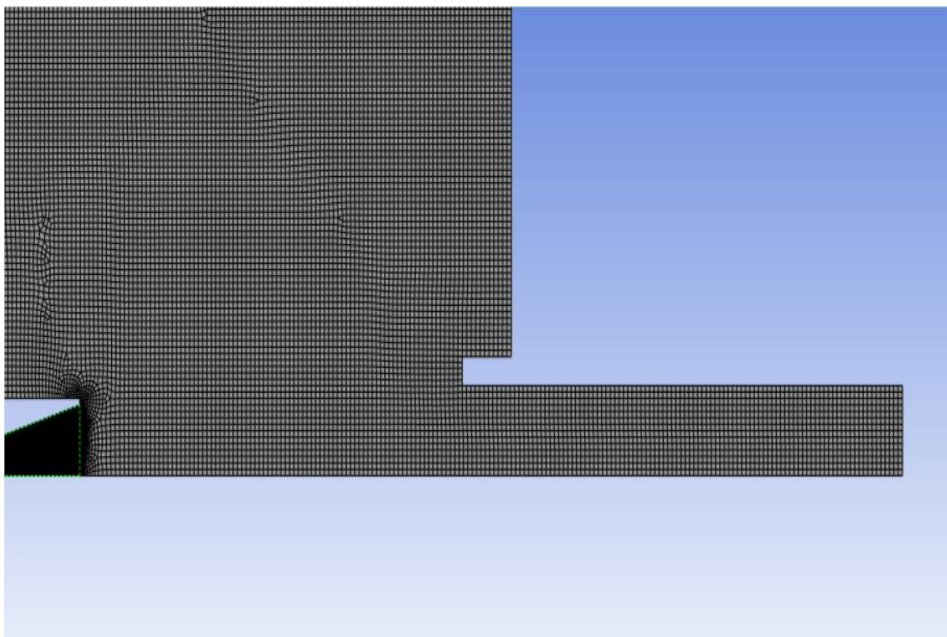


**Fig.9. Wall Meshing**

## 7. Ansys Fluent Set Up:

The contours ANSYS streamlined setup for evaluating jet nozzle flow. There are descriptions for geometry, mesh, physics models, boundary conditions, solver settings, and post-processing.

**Table 3. Ansys Fluent Set Up**

SL No.	Type	Details	Remarks
1.	Solver	Scheme	Density Based
		Velocity	Absolute
		Time	Steady
		2D Space	Axisymmetric
2.	Model	Energy Equation	On
		Viscosity	Inviscid
3.	Material	Fluid	Nitrogen
		Density	Constant
		Viscosity	Inviscid
4.	Boundary Condition	Inlet	Pressure Inlet
		Inlet Total Gauge Pressure (Pa)	3203000
		Outlet	Pressure Outlet
		Outlet Gauge Pressure (Pa)	101325
		Operating Conditions (Pa)	0
5.	Reference Values	Compute From	Inlet
6.	Initialization	Method	Standard Initialization
		Compute From	Inlet
7.	Monitors	Courant Number	5
8.	Data File Quantities	Velocity	Velocity Magnitude
			Axial Velocity
		Temperature	Total Temperature
		Pressure	Static Pressure
			Dynamic Pressure
			Total Pressure



## 5. EXPERIMENTAL ANALYSIS

The pressure analysis was conducted through extensive experimentation, and the detailed results are discussed in this chapter. In this study, the configuration and results obtained using a L/De ratio of 2 are presented for simplicity and clarity, with all values listed in the accompanying tables attached at the end.

Throughout the experiment, various L/De ratios were tested, and a clear trend was identified, which allowed us to draw meaningful conclusions from the study.

The test setup involved analyzing the pressure distribution along the surface of the Mobile Launch Platform (MLP). The MLP surface was divided into different circles of varied diameters which provided us with the locations for measuring the pressure along the top surface of the launchpad. Our main concentration was on the inner circles namely circles 1, 2, and 3. These circles have a diameter of 56, 74, and 90.

Notably, the pressure values obtained along all the circles gradually decreased as the circle diameter increased. When the L/De ratio reached 6, the deflector no longer played a significant role, and the entire flow directly impinged on the plate. For the cold flow test with a L/De ratio of 2, the highest-pressure region was observed in the innermost circle.

Furthermore, the study also revealed regions of negative pressure, providing valuable insights into the flow structure and the occurrence of stagnation bubbles. However, it is essential to note that the negative pressures should not exceed a value of negative 1 bar. Overall, the experiments shed light on the pressure distribution and flow characteristics under different L/De ratios, allowing us to gain a deeper understanding of the phenomenon at hand.

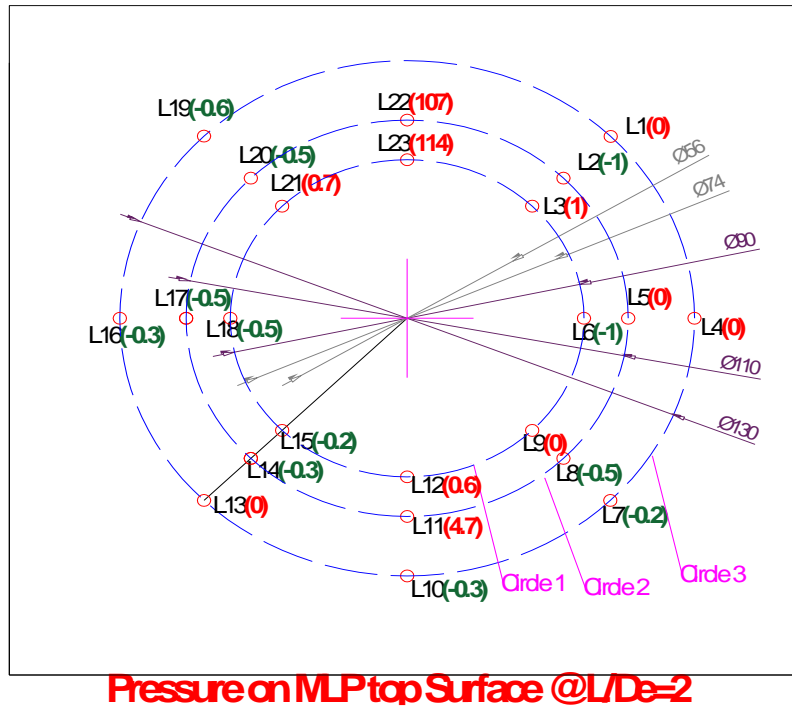


**Fig.9: Pressure obtained at the surface (All values are in mbar-G)**

**Table 4: Pressure obtained at MLP surface (All values in mbar-G)**

Location	Max Positive Pressure	Max Negative Pressure
Circle-1	114	-1
Circle-2	107	-1
Circle-3	-	-0.6

## 6. NUMERICAL ANALYSIS RESULTS

The experimental results for the CFD analysis on the launch pad have been widely discussed in this chapter. The summarized results are presented in a simplified way in the tables attached later. The configuration is tested at cold flow conditions keeping the chamber pressure constant at 32.03 bar and the operating condition of 101325 bar at the outlet. Another value that has been kept constant throughout the experiment is the specific heat ratio which is

valued at 1.4. The pressure contours at the wall are plotted which provides us with a better visualization of the problem statement.

## 1. Residuals:

The residuals were plotted and run till most of the equations reach a converge criterion of 0.001. The graphs contained x and y velocities along with the energy and continuity equations.

For different ratios, the number of iterations required to reach convergence was different but mostly attained a convergence within 20,000 iterations. This helps us to decide when to stop calculations and proceed to post-processing. For the ratio of 2, the residuals took 4,000 iterations to attain convergence. From the figure, it is evident that after 4,000 iterations the velocities and continuity graph converged. After convergence, we viewed the contours.

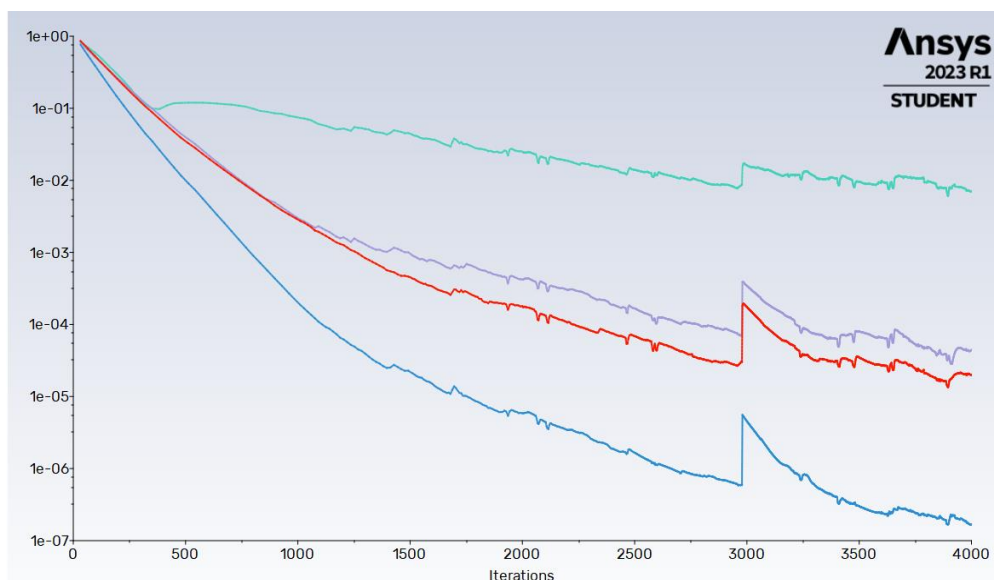


**Fig.10. Residual Contours**

## 2. Pressure Contours:

The static, dynamic, and total pressure were plotted using Ansys Fluent software. The flow can be satisfactorily observed in the dynamic pressure contour. The pressure contours show impingement in the wall properly.

**Table 5: CFD pressure obtained at the wall**

SL. NO.	RATIO	MAXIMUM PRESSURE	MINIMUM PRESSURE
1	2	872 mbar	-ve
2	4	900 mbar	-ve
3	6	1.01 bar	-ve



**Fig.11. Total Pressure Contour**

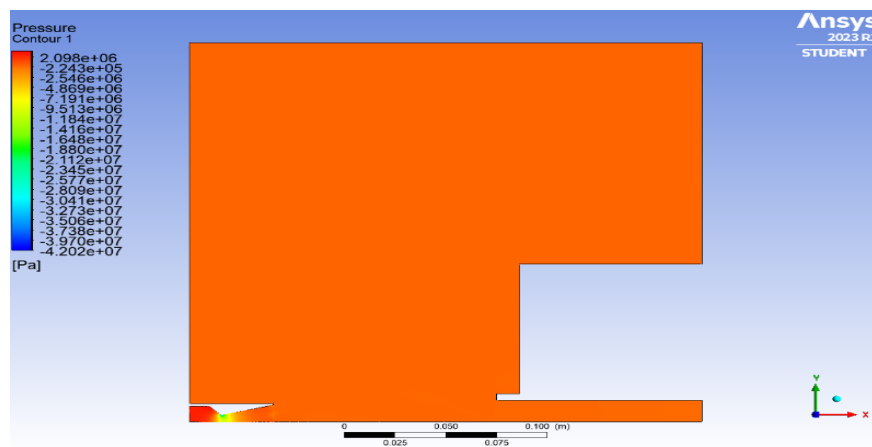


**Fig.12. Static Pressure Contour**

At the nozzle throat, the pressure is the maximum as there is minimum velocity. At the nozzle exit, an over-expanded flow can be seen and the nozzle flow is full. Although in the lower  $L/D_e$  ratios, the nozzle flow was overexpanded which can be easily understood from the fact that flow separation occurs at places downstream of the nozzle throat. As the cold flow test result is obtained it has been seen that most of the places except the nozzle are operating at atmospheric pressure conditions. This is easily understood that only the flow stream has a zone of higher pressures.

The wall pressures are our major concern. We can observe that the pressure at the walls parallel to the flow has more pressure than the walls present perpendicular to the flow. The place of impingement on the base shroud has the region of highest pressure in the wall region.

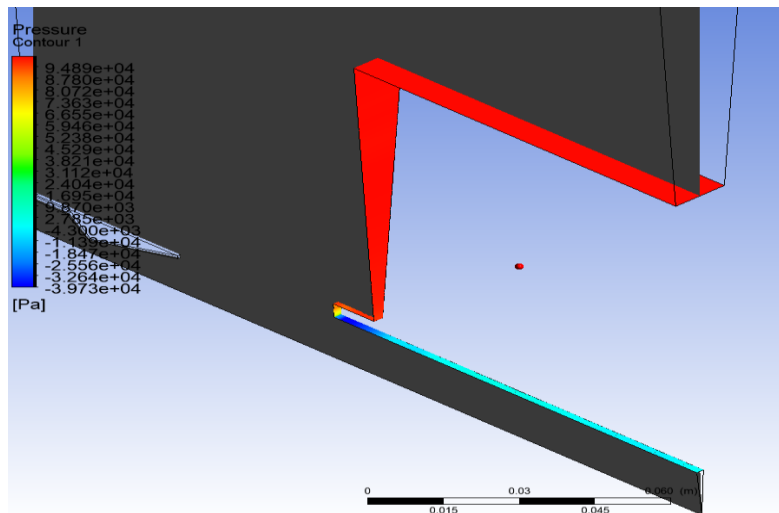


**Fig.13. Pressure at the wall**

The different  $L/De$  ratios have different pressures. The trend is observed that the pressure on the wall parallel to the flow direction has higher pressure zones than the walls perpendicular to the flow. This is because the shock strikes the impingement point which increases the pressure at that point. Increasing the  $L/De$  ratio increases the pressure impinging on the wall this in turn increases the force exerted by the jet on the wall.

Along the surface of the wall perpendicular to flow directions more or less the pressure is constant at 101325 bar. Zones of negative pressure were observed along the surface of the wall. This is due to the occurrence of separation bubbles at those zones. This provides us with a greater insight into the shock zone formations along the wall.

### **3. Temperature Contours:**

The temperature contour along the wall is also one of the main concerns as it helps to determine the thermodynamic heat transfer analysis along the surface of the wall. This helps us to provide a piece of knowledge about the heating of the surface of the MLP. The contour of the temperature well shows that the maximum flow of the exhaust plumes goes into the deflector and only a little part of it does impinge into the wall surface perpendicular to the flow of the jet.

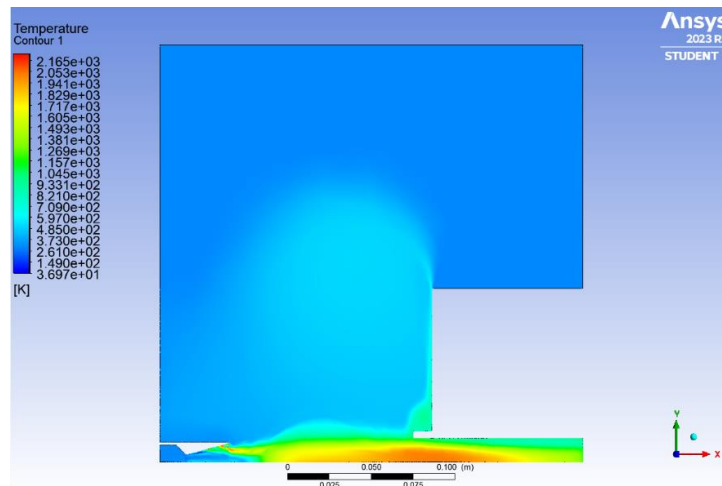


**Fig.14. Temperature Contour**

The wall temperatures of a cold flow experiment don't exceed more than 1000 K as the working fluid of nitrogen only reaches a maximum temperature of 600 K. As the flow impinges into the wall it heats up. For hot flow cases due to afterburning, this reason heats up to a large temperature.

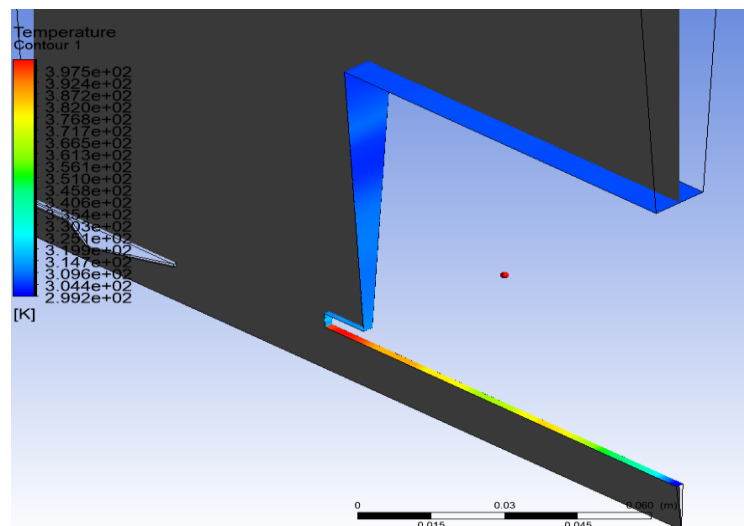


**Fig.15. Temperature at the wall**


The region inside the nozzle does not increase too much temperature only having 86.9 K at the nozzle exit.

**Table 6: CFD temperature obtained from the wall**

SL. NO.	RATIO	MAXIMUM TEMPERATURE (K)	MINIMUM TEMPERATURE (K)
1	2	402	300
2	4	476	300
3	6	560	300

#### 4. Velocity Contours:

Velocity  
Contour 1



A velocity contour plot showing the flow field around a rectangular obstacle. The plot is titled "Velocity Contour 1". A color bar on the left indicates velocity values in  $\text{m s}^{-1}$ , ranging from 0.000e+00 (blue) to 9.182e+03 (red). The plot shows a high-velocity region (red) entering from the left, which is deflected and accelerated around the obstacle. A small inset shows a zoomed-in view of the flow near the bottom-left corner of the obstacle. A coordinate system in the bottom right shows the x and y axes.

9.182e+03  
8.699e+03  
8.215e+03  
7.732e+03  
7.249e+03  
6.766e+03  
6.282e+03  
5.799e+03  
5.316e+03  
4.833e+03  
4.349e+03  
3.866e+03  
3.383e+03  
2.900e+03  
2.416e+03  
1.933e+03  
1.450e+03  
9.665e+02  
4.833e+02  
0.000e+00

[m s<sup>-1</sup>]

0 0.050 0.100 (m)

0.025 0.075

y

x

31 | Page

Along the wall, the velocity contour obtained was 0 m/s as the wall operating conditions specified were no-slip conditions. The local velocity contour shows uniformity in the contour.

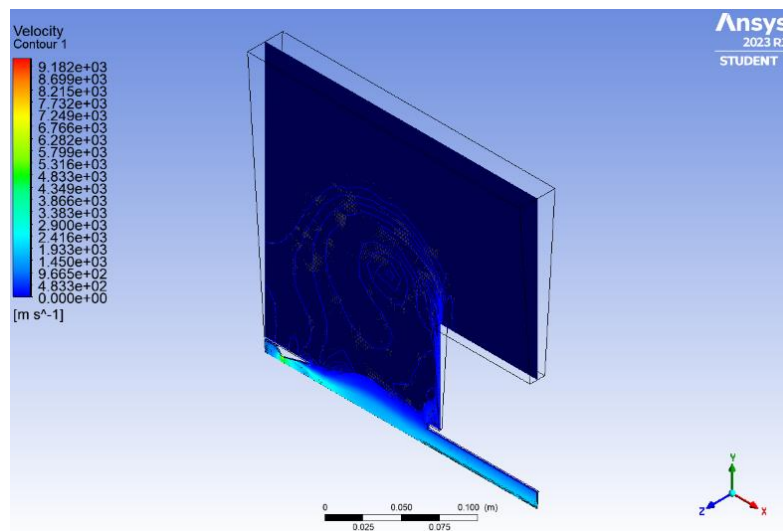


**Fig.18. Velocity Magnitude Contour**

## CONCLUSION

The MLP surface has a wide range of applications that are required to launch a vehicle. The vehicle imparts pressure on the surface of the MLP which helps the vehicle to gain lift-off momentum. The simplicity and practicality of the launch pad make it advantageous to mitigate its usage for launching purposes.

High-velocity and high-temperature exhaust gases make it challenging to design the launchpad. The experimental analysis was carried out in the JATF facility which brings us to conclude with the comparison with the CFD results.

The results are concluded for the  $L/D_e$  ratio of 2 and nozzle having exit Mach Number of 3.5: -

1. For the lower  $L/D_e$  ratios the impingement occurs very less on the surface perpendicular to the wall. The maximum flow passes through the cut-out to the jet deflector.
2. The values obtained at the wall decrease as we go further away from the center of the structure. These values obtained can be best compared with the CFD results as the values obtained at the inner circle of the MLP surface are more or less the same as that obtained in the CFD results.
3. The nozzle was at full flowing condition during the experiment but the CFD results don't correspond to it. This happened due to less computational power and coarse mesh size.



4. The pressure obtained was profoundly affected by the height at which the nozzle is raised. The pressure imparted on the wall increased to 872 mbar in the case of CFD results till the  $L/D_e$  ratio of 2. Similarly, the  $L/D_e$  ratio is 2, and the results obtained at the experiment were increased to 114 mbar-G at the innermost circle.

## REFERENCE

- [1] G. R. Rao, U. S. Ramakanth, A. Lakshman, “Flow Analysis in a Convergent-Divergent Nozzle Using CFD”, International Journal of Research in Mechanical Engineering, vol. 1, issue 2, pp. 136-144, 2013.
- [2] NUMERICAL SIMULATION OF SUPERSONIC JET IMPINGEMENT Afq Radzman, Naseem Uddin Universiti Teknologi Brunei, Jalan Tungku Link, Gadong, BE1410
- [3] Gummer, J. H. and Hunt, B. L.: ‘The impingement of a uniform, axisymmetric, supersonic jet on a perpendicular flat plate’, In The Aeronautical Quarterly, Bristol, 1921, pp. 403-420.
- [4] A review of impinging jets during rocket launching Chongwen Jiang\* , Tianyixing Han, Zhenxun Gao, Chun-Hian Lee National Laboratory for Computational Fluid Dynamics, School of Aeronautic Science and Engineering, Beihang University, 100191, Beijing, China
- [5] N. Tsuboi, A.K. Hayashi, T. Fujiwara, K. Arashi, M. Kodama, Numerical simulation of supersonic jet impingement on a ground, SAE Trans. 100 (1) (1991) 2168–2180.
- [6] C.D. Donaldson, R.S. Snedeker, A study of free jet impingement. Part 1. Mean properties of free and impinging jets, J. Fluid Mech. 45 (2) (1971) 281–319.
- [7] 1. G. SATYANARAYANA, 2. Ch. VARUN, 3. S.S. NAIDU CFD ANALYSIS OF CONVERGENT-DIVERGENT NOZZLE 1-3. DEPARTMENT OF MECHANICAL ENGINEERING, MVGRCE, VIZIANAGARAM, 535005, (A.P.), INDIA
- [8] AIAA 95-2935 Experiments on the Flow Over a Flat Surface Impinged by a Supersonic Jet A. M. Al-Qutub and M. O. Budair King Fahad University of Petroleum & Minerals Dhahran, Saudi Arabia
- [9] Experimental Study of Underexpanded Supersonic Jet Impingement on an Inclined Flat Plate Yusuke Nakai,\* Nobuyuki Fujimatsu,†, and Kozo Fujii‡
- [10] Fujii, K., Tsuboi, N., and Fujimatsu, N., “Visualization of Jet Flows over a Plate by Pressure—Sensitive Paint Experiments and Comparison with CFD,” Visualization and Imaging in Transport Phenomena, Vol. 972, New York Academy of Sciences, New York, 2002, pp. 265– 270.